CHEMISTRY OF MATERIALS
Article

Chem. Mater. **2009,** *21,* 2763–2769 2763
DOI:10.1021/cm900289c

One-Pot Route to Produce Hierarchically Porous Titania Thin Films by Controlled Self-Assembly, Swelling, and Phase Separation

Luca Malfatti,[†] Martín G. Bellino,[‡] Plinio Innocenzi,*[,†] and Galo J. A. A. Soler-Illia*[,‡,§]

[†]*Laboratorio di Scienza dei Materiali e Nanotecnologie, D.A.P., Università di Sassari, CR-INSTM Palazzo del Pou Salit, Piazza Duomo 6, 07041 Alghero (SS), Italy,* [‡]*Gerencia de Química, Centro Atómico Constituyentes, Comisión Nacional de Energía Atómica, Avenida General Paz 1499 (B1650KNA) San Martín, Provincia de Buenos Aires, Argentina and Centro Interdisciplinario de Nanociencia y Nanotecnología, Avenida Rivadavia 1917, Buenos Aires C1033AAJ, Argentina, and* [§]*DQIAyQF, FCEN, Universidad de Buenos Aires, Ciudad Universitaria, Pabellón II, C1428EHA, Buenos Aires, Argentina and CONICET, Avenida Rivadavia 1917, Buenos Aires C1033AAJ, Argentina*

Received January 30, 2009. Revised Manuscript Received March 5, 2009

Expanding mesopore size beyond a 10 nm diameter is a big challenge for developing applications based on mesostructured-mesoporous thin films, especially in nanobiotechnology. This triggers the need of new multipore materials produced by reproducible soft chemistry routes. We present here a novel and simple one-pot synthesis method that allows the creation of a new kind of hierarchically porous thin film using a combination of supramolecular templating and phase separation. Accurate tuning of pore size distribution (bimodal, with small mesopores 13−18 nm diameter, and large pores 20−150 nm diameter) is attained by controlling the solubility of a pore enhancement agent, poly (propylene glycol), in the presence of a co-solvent. The reported strategy permits the in situ tuning of the processes that govern the pore generation at different length scales; this opens a path for fabrication of multimodal mesoporous films, which represents an important breakthrough in the field.

Introduction

Fabrication of complex nanoscale porous materials through the co-assembly of inorganic and organic species is a current trend in chemistry and nanomaterials science.[1,2] Mesoporous thin films represent an example of highly organized porous materials, the synthesis of which is achieved through a combination of sol−gel and supramolecular chemistry.[3,4] Ordered mesoporous materials obtained by micelle templating have a monodisperse pore diameter which is generally restricted within the 2−10 nm range,[5] well below the 50 nm upper limit defined by IUPAC. This "10 nm barrier" represents, therefore, a severe limitation for developing novel applications of ordered mesoporous thin films, such as those in nanobiotechnology, for immobilization of biomolecules,[6] large-molecule catalysis or sensing. This limitation triggers the need of new multipore materials produced by reproducible soft chemistry routes.[7] Although the evaporation induced self-assembly (EISA) method is a very flexible and well developed synthesis route,[8] so far, large pores (up to 50 nm) have only been obtained in ultrathin oxide films by using custom-designed polymer templates and very dilute precursor concentrations. In these conditions, template micelles seem to spread over the substrate and exhibit a higher range of open porosities; these pores can be better defined as craters in patterned monolayers,[9] whose size can be controlled as a function of the molecular weight of the template.[10] These examples are, however, limited to pore monolayers or bilayers, or even arranged craters.[11]

Hierarchical porous structures, presenting nested pores with different sizes and functions, represent a natural

*To whom correspondence should be addressed. E-mail: plinio@uniss.it (P.I.), gsoler@cnea.gov.ar (G.J.A.A.S.-I.).

(1) See, for example, Special Issue: Templated Materials; Jaroniec, M., Schüth, F., Eds.; Chem. Mater. 2008, 20, 599−600.
(2) Soler-Illia, G. J. A. A.; Sanchez, C.; Lebeau, B.; Patarin, J. *Chem. Rev.* **2002**, *102*(11), 4093.
(3) Sanchez, C.; Boissière, C.; Grosso, D.; Laberty, C.; Nicole, L. *Chem. Mater.* **2008**, *20*, 682.
(4) (a) Shi, J. L.; Hua, Z. L.; Zhang, L. X. *J. Mater. Chem.* **2004**, *14*, 795. (b) Nicole, L.; Boissière, C.; Grosso, D.; Quach, A.; Sanchez, C. *J. Mater. Chem.* **2005**, *15*, 3598. (c) Soler-Illia, G. J. A. A.; Innocenzi, P. *Chem.—Eur. J.* **2006**, *12*, 4478.
(5) Soler-Illia, G. J. A. A.; Crepaldi, E. L.; Grosso, D.; Sanchez, C. C. *Curr. Opin. Colloid Interface Sci.* **2003**, *8*, 109.
(6) Yiu, H. H. P.; Wright, P. A. *J. Mater. Chem.* **2005**, *15*, 3690.
(7) Tortajada, M.; Ramón, D.; Beltrán, D.; Amorós, P. *J. Mater. Chem.* **2005**, *15*, 3859.
(8) (a) Lu, Y.; Ganguli, R.; Drewien, C.; Anderson, M.; Brinker, C. J.; Gong, W.; Guo, Y.; Soyez, H.; Dunn, B.; Huang, M.; Zink, J. *Nature* **1997**, *389*, 364. (b) Brinker, C. J.; Lu, Y.; Sellinger, A.; Fan, H. *Adv. Mater.* **1999**, *11*, 579.
(9) (a) Fischer, A.; Kuemmel, M.; Järn, M.; Lindén, M.; Boissière, C.; Nicole, L.; Sanchez, C.; Grosso, D. *Small* **2006**, *4*, 569. (b) Kuemmel, M.; Allouch, J.; Nicole, L.; Boissière, C.; Laberty, C.; Amenitsch, H.; Sanchez, C.; Grosso, D. *Chem. Mater.* **2007**, *119*, 3717.
(10) Brezesinski, T.; Groenewolt, M.; Gibaud, A.; Pinna, N.; Antonietti, M.; Smarsly, B. M. *Adv. Mater.* **2006**, *18*, 2260.
(11) (a) Cheng, Y.-J.; Müller-Buschbaum, P.; Gutmann, J. S. *Small* **2007**, *3*, 1379. (b) Cheng, Y.-J.; Zhou, S.; Gutmann, J. S. *Macromol. Rapid Commun.* **2007**, *28*, 1392.

Published on Web 05/21/2009

evolution of advanced nanoporous materials. [12−19] The possibility of obtaining such hierarchical structures through "one-pot" assembly processes is a tempting challenge so far. Crossing the "10 nm barrier" in mesoporous self-assembled films, and obtaining at the same time an accurate control of the pore size, up to a hierarchical and multimodal pore distribution, represents an important breakthrough in the field. Previous reports of hierarchically porous films rely on a combination of techniques. Yang et al. demonstrated the possibility of producing three-length-scale templated oxide films (silica, niobia, or titania) by the combined use of micromolding, latex beads, and surfactant templating.[12a] Macro-mesoscale templated films or gels can also be obtained by concurrent sol−gel transition and phase separation, which can be induced by the incorporation of supramolecular templates or polymers. In this case, macropores arise from phase separation, and small-size mesopores (∼2−3 nm) are generated after the elimination of polymers strongly embedded into a sol−gel matrix.[20,21] The use of functional nanoparticles as inorganic precursors has been also reported; macro-mesoporous ceria can be generated by phase separation processes induced by the presence of a functional polymer.[22] More recently, the use of breath figures processing (high humidity conditions) in combination with functional nanobuilding blocks allowed preparing a wide range of nanoparticle-based macro-mesoporous thin films.[23] In these two cases, mesopores are generated from the textural porosity derived from interparticle spaces; therefore, the mesopore range is limited by the nanoparticle precursor size.

In the present work we present for the first time to our knowledge, a simple and reproducible one-pot synthesis route to produce titania thin films with hierarchical porous structures, formed by nested meso- and macropores, with diameters controllable in the 10−200 nm range. A fine-tuning of the pore size is attained through the control of the synthesis parameters. We have used a triblock copolymer template, Pluronic F127, combined with a pore enhancing agent, poly(propylene glycol) (PPG); this strategy permits monomodal or multimodal pore systems to be obtained. We selected the different precursor compounds on the basis of a specific design of the solution; we have used a low-weight (MW ≈ 4000) simple polymer such as PPG as a molecule that swells the template micelles at lower concentrations or that induces a phase separation at higher concentrations. Butanol was used as a solvent to adequately dissolve PPG; Pluronic F127, besides being the templating agent during self-assembly, plays also a fundamental role in increasing the solubility of PPG. This approach is simple and employs commercial, low cost, and easily removable templating agents. We have systematically changed the synthesis parameters, such as the relative amount of the templates, the content of water and tetrahydrofuran (THF) co-solvent, to modulate the pore size and pore distribution. The films show a high tuning in terms of their porosity properties; large mesopores or bimodal porous distribution can be obtained as a function of the synthesis parameters. These films can be easily deposited on silicon and glass substrates without cracking and maintaining a high optical transparency. In addition, titania films are useful for molecule or ion trapping,[24] selective molecule detection,[25] catalysis, photocatalysis,[26] and dye-sensitized solar cells.[27] Titania is also known to be stable in aqueous solutions, under conditions comparable to biological media, where mesoporous silica stability is limited.[28] This last feature is important for applications in nanobiotechnology (microarrays, ultrasensitive detection, molecule imaging) or nanomedicine (controlled delivery, implants).

Experimental Section

$TiCl_4$ (99.9%, Aldrich), triblock copolymer Pluronic F127 ($PEO_{106}-PPO_{70}-PEO_{106}$) (Aldrich), poly(propylene glycol) PPG (PPO_{68}, MW ≈ 4000) and THF were purchased from Aldrich, butanol (BuOH) was purchased from Ciccarelli (Argentina). All the reagents were used without further purification.

Typically, the precursor sols containing the titania source were prepared by adding, in the following order, 14.6 cc of BuOH, 0.44 cc of $TiCl_4$ and Pluronic F127. After 5 min stirring, 0.72 cc of water and PPG were added to obtain the solutions for film preparation; solutions were prepared under ordinary laboratory conditions, at 298 K and atmospheric pressure, and stored in closed glass or plastic bottles. Butanol was used as the solvent because of its excellent substrate wetting, slow evaporation rate, and ability to

(12) (a) Yang, P.; Deng, T.; Zhao, D. Y.; Feng, P.; Pine, D.; Chmelka, B. F.; Whitesides, G. M.; Stucky, G. D. *Science* **1998**, *282*, 2244. (b) Zhao, D.; Huo, Q.; Feng, J.; Chmelka, B. F.; Stucky, G. D. *J. Am. Chem. Soc.* **1998**, *120*, 6024.
(13) Nakanishi, K.; Tanaka, N. *Acc. Chem. Res.* **2007**, *40*, 863.
(14) Fujita, S.; Nakano, H.; Ishii, M.; Nakamura, H.; Inagaki, S. *Microporous Mesoporous Mater.* **2006**, *96*, 205.
(15) Kuang, D.; Brezesinski, T.; Smarsly, B. *J. Am. Chem. Soc.* **2004**, *126*, 10534.
(16) Brandhuber, D.; Torma, V.; Raab, C.; Peterlik, H.; Kulak, A.; Hüsing, N. *Chem. Mater.* **2005**, *17*, 4262.
(17) Li, F.; Wang, Z.; Ergang, N. S.; Fyfe, C. A.; Stein, A. *Langmuir* **2007**, *23*, 3996.
(18) Grosso, D.; Soler-Illia, G. J. A. A.; Crepaldi, E. L.; Charleux, B.; Sanchez, C. *Adv. Funct. Mater.* **2003**, *13*, 37.
(19) Sel, O.; Kuang, D.; Thommes, M.; Smarsly, B. *Langmuir* **2006**, *22*, 2311.
(20) Kumon, S.; Nakanishi, K.; Hirao, K. *J. Sol-Gel Sci. Technol.* **2000**, *19*, 1573.
(21) Fuertes, M. C.; Soler-Illia, G. J. A. A. *Chem. Mater.* **2006**, *18*, 2109.
(22) Bouchara, A.; Soler-Illia, G. J. A. A.; Chane-Ching, J.-Y.; Sanchez, C. *Chem. Commun.* **2002**, 1234.
(23) Sakatani, Y.; Boissière, C.; Grosso, D.; Nicole, L.; Soler-Illia, G. J. A. A.; Sanchez, C. *Chem. Mater.* **2008**, *20*, 1049.
(24) (a) Angelomé, P. C.; Aldabe-Bilmes, S.; Calvo, M. E.; Crepaldi, E. L.; Grosso, D.; Sanchez, C.; Soler-Illia, G. J. A. A. *New J. Chem.* **2005**, *29*, 59. (b) Angelomé, P. C.; Soler-Illia, G. J. A. A. *Chem. Mater.* **2005**, *17*, 322.
(25) Otal, E. H.; Angelomé, P. C.; Aldabe-Bilmes, S.; Soler-Illia, G. J. A. A. *Adv. Mater.* **2006**, *18*, 934.
(26) (a) Sakatani, Y.; Grosso, D.; Nicole, L.; Boissière, C.; Soler-Illia, G. J. A. A.; Sanchez, C. *J. Mater. Chem.* **2006**, *16*, 77–82.(b) Angelomé, P. C.; Andrini, L.; Calvo, M. E.; Requejo, F. G.; Bilmes, S. A.; Soler-Illia, G. J. A. A. J. Phys. Chem. C 2007, *111*, 10886, and references therein.
(27) (a) Malfatti, L.; Falcaro, P.; Amenitsch, H.; Caramori, S.; Argazzi, R.; Bignozzi, C. A.; Enzo, S.; Maggini, M.; Innocenzi, P. *Microporous Mesoporous Mater.* **2006**, *88*, 304. (b) Lancelle-Beltran, E.; Prené, P.; Boscher, C.; Belleville, P.; Buvat, P.; Lambert, S.; Guillet, F.; Boissière, C.; Grosso, D.; Sanchez, C. *Chem. Mater.* **2007**, *19*, 4349.
(28) Bass, J. D.; Grosso, D.; Boissière, C.; Belamie, E. T.; Coradin; Sanchez, C. *Chem. Mater.* **2006**, *18*, 6152.

dissolve PPG (this polymer is much less soluble in other volatile solvents such as ethanol). The relative concentrations of Pluronic F127 and PPG were systematically changed to optimize the synthesis parameters. Molar ratios for the precursor sols were $TiCl_4/BuOH/H_2O/PPG/F127 = 1:40:10:P:S$, where P = [PPG]/[Ti] and S = [F127]/[Ti]. P was varied between 0 and 2.25×10^{-2} and S between 4×10^{-3} and 1.6×10^{-2}. When THF was added to the solutions, V_{THF} is defined as the percentage volume ratio between the volume of THF and the final volume of the solution. V_{THF} was systematically varied between 0% and 37%. An intense orange color is observed in solutions containing Ti(IV) upon THF addition, indicating formation of the well-known Ti(IV) chloride-THF complex.

Titania films were produced by dip-coating at a withdrawal speed of 0.5 mm s^{-1}. Silicon substrates were pretreated by a 5 min immersion in KOH ethanol solution (10% m/m), followed by 5 min immersion in chromic acid, and subsequent thorough rinsing with distilled water, to improve wetting. Prior to deposition, soda-lime glass slides (75 mm long × 25 mm wide) or silicon wafer substrates (75 mm long × 10 mm wide) were thoroughly washed with Dextran or other suitable surfactant-based cleaning agent, followed by successive rinsing in water, ethanol, and acetone. The relative humidity (RH) during dip-coating was set at 20%. Post-treatment of these films was performed following previously reported procedures that lead to reproducible mesoporous titania.[29] After deposition, films were aged at RH 50% for 24 h and then dried in an oven at 60 and 130 °C (24 h at each temperature). Finally, the samples were calcined in air at temperatures between 130 and 350 °C (1 °C min^{-1} ramp) with a final 2 h step at 350 °C. At this final temperature, robust films with excellent adhesion to the substrate (i.e., they were not detached after peeling off Scotch tape at 90°) and well-defined mesoporous structure are obtained.

Film thickness and density were obtained from the analysis of critical angle by X-ray Reflectometry (XRR) measurements performed at the D10A-XRD2 line of Laboratório Nacional de Luz Síncrotron, Campinas, SP, Brazil (λ = 1.5498 Å). To obtain accurate density values, measurements were done at low humidity, to avoid atmospheric water condensation within the pores that leads to underestimation of mesoporosity.[30] Film thickness of samples deposited on silicon substrates were also measured by an Alpha-Spectroscopic Ellipsometry (α-SETM) instrument (J.A.Woollam, U.S.A.). The data were fitted using a Cauchy film model.

Film mesostructure was analyzed using Small Angle X-ray Scattering (SAXS) on glass cover-supported films at the D11A-SAXS2 line of LNLS, Campinas, SP, Brazil (λ = 1.608 Å) at normal (90°) and glancing (3°) incidence.

Field Emission-Scanning Electron Microscopy (FE-SEM) images were taken with a ZEISS LEO 982 GEMINI field emission electron microscope in the secondary-electron mode, using an in-lens detector to improve resolution.

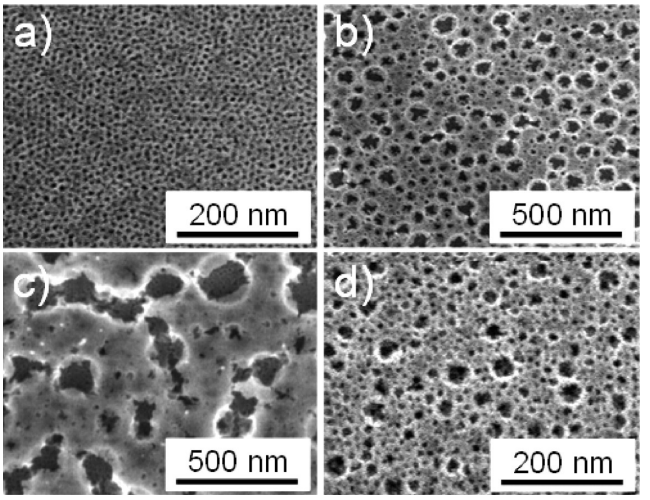

Figure 1. FE-SEM micrographs of typical self-assembled hierarchical titania porous films. The samples have been prepared starting from different precursor solutions (see Experimental Section for more details): (a) $P = 0$, $S = 4 \times 10^{-3}$, $V_{THF} = 0\%$; (b) $P = 1.5 \times 10^{-2}$, $S = 4 \times 10^{-3}$, $V_{THF} = 29\%$; (c) $P = 1.5 \times 10^{-2}$, $S = 4 \times 10^{-3}$, $V_{THF} = 0\%$; (d) $P = 1.5 \times 10^{-2}$, $S = 4 \times 10^{-3}$, $V_{THF} = 37\%$.

Pore size analysis and statistic were done with software for image analysis (ImageJ).

Optical transmittance of porous films was measured on soda-lime glass slides with a Hewlett-Packard 8453 spectrophotometer in transmission mode.

Results and Discussion

Under the synthesis conditions explored here (see Experimental Section), uniform and highly transparent films can be obtained (UV−vis spectra are shown in the Supporting Information). The films have been deposited by dip-coating at low withdrawal rates that allowed producing crack-free thin films with excellent adhesion to substrates in a reproducible way. Figure 1 shows some typical FE-SEM micrographs that illustrate the variety of mesoporous structures achievable with this approach by adjusting relevant synthesis parameters such as the presence of a pore enhancing agent or a co-solvent. We observed that the porous structure of the titania films is dramatically affected by a change in the relative amounts of PPG and THF in the starting solutions.

Figure 1a shows a top-view of a film sample obtained from a butanol solution containing $TiCl_4$, water (h = $[H_2O]/[Ti]$ = 10) and Pluronic F127, with no addition of PPG or THF; under these conditions, similar to those reported for pure mesoporous titania films,[30] a homogeneous pore structure with a local hexagonal organization is obtained, as suggested by SAXS information. Radially integrated patterns at 90° incidence of this "blank" sample show the presence of a well-defined peak, which corresponds to an in-plane center-to-center distance of d = 13.5 nm (see below). Addition of PPG and THF to the same precursor solution results in the appearance of a bimodal distribution of pores. A population of smaller pores with diameters centered at 15 nm and larger pores with an average diameter of 90 nm are observed (Figure 1b). Higher concentrations of PPG in the absence of THF produce

(29) (a) Crepaldi, E. L.; Soler-Illia, G. J. A. A.; Grosso, D.; Cagnol, F.; Ribot, F.; Sanchez, C. *J. Am. Chem. Soc.* **2003**, *125*, 9770. (b) Crepaldi, E. L.; Soler-Illia, G. J. A. A.; Grosso, D.; Sanchez, C. *New J. Chem.* **2003**, *27*, 9.
(30) Van der Lee, A. *Solid State Sci.* **2000**, *2*, 257.
(31) Choi, S. Y.; Lee, B.; Carew, D. B.; Mamak, M.; Peiris, F. C.; Speakman, S.; Chopra, N.; Ozin, G. A. *Adv. Funct. Mater.* **2006**, *16*, 1731.

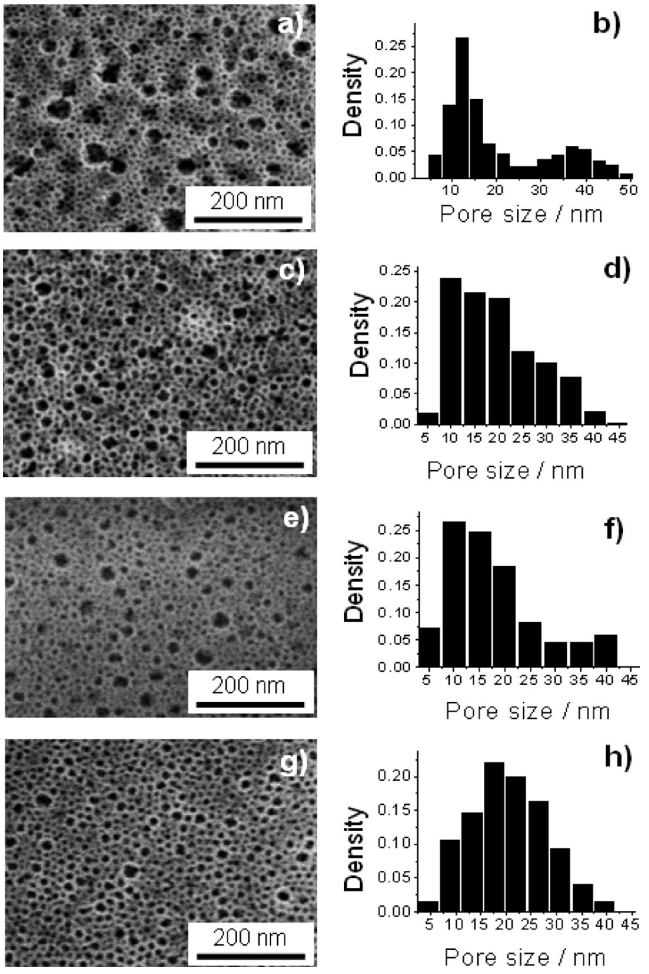

Figure 2. FE-SEM micrographs and relative pore size distributions of samples prepared as a function of V_{THF} maintaining constant the other synthesis parameters ($P = 6.25 \times 10^{-3}$, $S = 4 \times 10^{-3}$): (a) $V_{THF} = 0\%$; (c) $V_{THF} = 17\%$; (e) $V_{THF} = 29\%$; (g) $V_{THF} = 37\%$.

even larger pores (150−200 nm diameter, Figure 1c) that coexist with smaller mesopores and tend toward coalescence. The addition of THF to the latter system allows, as a general trend, to control the pore size distribution and dimension. When this co-solvent is added, two populations of well-defined pores with diameters 15 and 35 nm are obtained (Figure 1d). A preliminary observation of these systems suggests that the presence of two different pore populations can be due to two different processes taking place concurrently upon film formation and processing: mesoscale templating and phase separation.

Pore sizes and distribution can be finely controlled by changing the external synthesis parameters. Figure 2 shows the dramatic effect of the THF amount added to the precursor solution on the film porosity for PPG-containing systems. We prepared samples with fixed contents of F127 and PPG ($P = 6.25 \times 10^{-3}$, $S = 4 \times 10^{-3}$) and variable amount of THF. V_{THF} is defined as the relative volume of THF with respect to the total precursor solution volume. In this case, in the absence of THF, a bimodal pore distribution is reproducibly obtained throughout the samples. Panels a and b of Figure 2 show a small pore population with center-to-center interpore distance (d_{ip}) peaking at 15 nm and a well-defined fraction of larger mesopores with

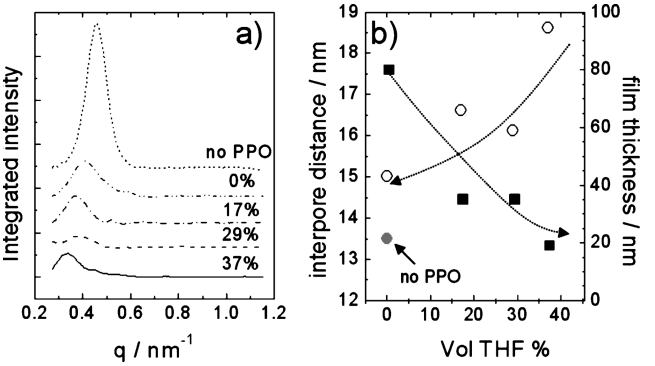

Figure 3. (a) Integrated intensity of SAXS patterns at normal incidence as a function of V_{THF}; (b) Interpore distance (○, estimated by SAXS) and film thickness (■, estimated by ellipsometry and XRR) as a function of V_{THF}. The data are referred to the same series of Figure 2. The dotted curve in panel a and the gray dot value in panel b correspond to the reference sample shown in Figure 1a. The dotted arrows are a guide for the eye.

38 nm average diameter. The larger pores are evident on the film surface, and the lower dimension mesopores decorate the walls. For larger V_{THF} values (panels c−f of Figure 2), a continuous change in the pore system morphology is observed, and both pore distributions partially overlap, attaining closer diameter values. In the extreme of $V_{THF} = 37\%$, a large distribution of mesopores, with average diameter centered at 20 nm is obtained (panels g, h of Figure 2).

2D-SAXS patterns showed rings at 90° incidence on glass cover supported films; the well-defined signals are indicative of pore order at the mesoscale. The values obtained from SAXS correspond to the interpore distances (d_{ip}); an excellent agreement is found between the d_{ip} values obtained by SAXS and those obtained by SEM image analysis of the smaller pores.[32] Patterns collected at 3° incidence show weak signals because of the low quantity of matter; the patterns are indicative of local pore organization; the scattering intensity of the SAXS patterns decreases in intensity with the increase of V_{THF}. Figure 3a shows the integrated intensity of 90° incidence SAXS data of the same series of films shown in Figure 2; the pattern of a titania film without PPG and THF is reported as a reference. The SAXS results show that a higher amount of THF in the precursor solution results in lower scattering and a shift of the scattering angle to lower q values, reflecting a higher average d_{ip} (Figure 3b). Film thickness determined by ellipsometry, cross-section FE-SEM, and XRR decreases with increasing V_{THF}, as also shown in Figure 3b. The smaller quantity of matter deposited with increasing dilution explains the observed trend in scattering intensity.

The size of the large pore population is also dependent on V_{THF}; this feature, in combination with the SAXS analysis of the smaller pores, suggests that the interplay of PPG and THF is a determinant in the solubility of PPG in the micelles, which seems to be a crucial parameter in pore size control (see below).

(32) It is important to stress that under our SAXS conditions (camera length 584 mm), any periodic feature larger that 25 nm cannot be detected, for it falls inside the beam stopper.

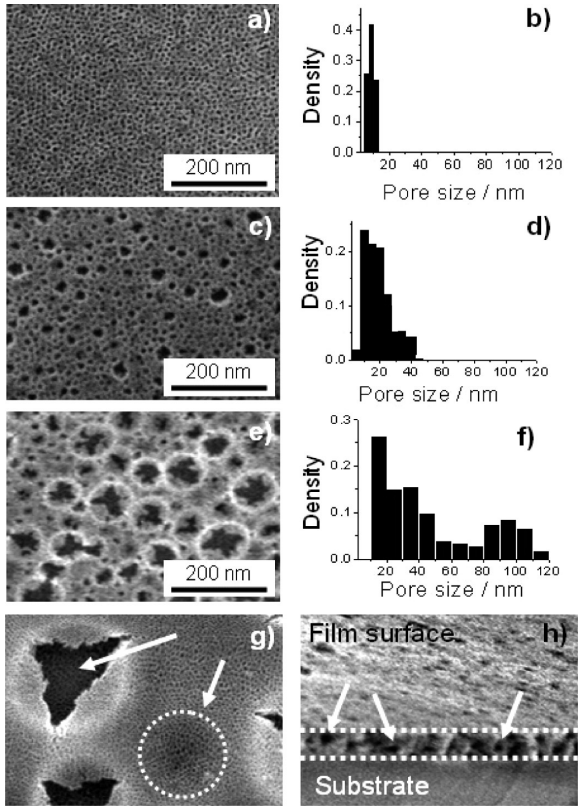

Figure 4. (a−f) FE-SEM micrographs and relative pore size distributions of samples prepared as a function of P maintaining constant the other synthesis parameters ($S = 4 \times 10^{-3}$, $V_{THF} = 29\%$): (a) $P = 0$; (c) $P = 6.25 \times 10^{-3}$; (e) $P = 1.5 \times 10^{-2}$. (g) Detail of a FE-SEM micrograph that shows small pores (arrow) and large pores (dotted circles) beneath the first porous layer. The circle diameter is around 200 nm. (h) FE-SEM cross section of a 80 nm thick film. The white arrows indicate macropores along the film thickness.

Figure 4 shows the effect of increasing PPG quantities for systems with a constant $V_{THF} = 29\%$; no large mesopores are observed in the absence of the pore enhancing agent (Figure 4a and 4b). Addition of small amounts of PPG ($P = 6.25 \times 10^{-3}$) leads to an increase in the size of the smaller mesopores, the interpore distance increasing from 13.5 to 15 nm, according to FE-SEM and SAXS. In addition, a population of large pores of 30−40 nm diameter appears in these conditions (panels c,d of Figure 4). For higher PPG added quantities, the diameter of the small mesopore population remains around 16 nm, almost reaching a plateau. On the other hand, the average diameter of the large pore population increases in a sustained way, to about 100 nm (panels e,f of Figure 4), and to more than 200 nm for higher PPO concentrations (not shown). In some cases, a third population of pores is observed, producing complex "flower-like" patterns such as those shown in the Table of Contents illustration. It is interesting to remark that the films are not formed by a monolayer of large mesopores; a close FE-SEM examination of the surface in Figure 4g reveals that a mesoporous layer is present beneath the large pore openings. The same phenomenon has been observed in all the bimodal pore size samples, which display a hierarchical structure where the large pore population (> 80 nm) is generally connected by the smaller pores. A second important point is that the large mesopores are not restrained to the surface; FE-SEM images in Figure 4g (surface view detail) and in Figure 4h (cross section view) of the 80 nm thick films show that both mesopore populations coexist all along the film thickness. In the particular case of Figure 4h, directly interconnected large pores can be observed.

The information collected in Figures 2, 3, and 4 demonstrates that the presented method allows the production of titania thin films with homogeneously dispersed large pore size, permitting a fine-tuning of the porosity in terms of the pore size and monomodal/bimodal distribution by varying V_{THF} and PPG concentration. It is also clear from these experiments that the presence of PPG influences the size of mesopores at two different length scales. The information presented in Figure 4, in particular, reinforces the hypothesis that the role of PPG is crucial in the development of the larger pore population, probably by triggering a phase separation process.

The observed crossed effect of the co-solvent and PPG in the swelling of the smaller mesopores suggests a complex synergy between these two components. Figure 5 summarizes the interpore distances for the smaller pore population (Figure 5a) and the pore size diameters (Figure 5b) of the studied samples, obtained from the analysis of SAXS and FE-SEM data. The global trends in pore size are now clearly observed when data are organized in this representation. Addition of PPO at $V_{THF} < 20\%$ results in an appreciable swelling of the small pores, until a leveling off at a 16 nm interpore distance; this saturation of pore size is related to a limited solubility of PPG in the F127 micelles. At the same time, larger mesopores begin to appear; their average size is controlled by the PPO concentration. For $V_{THF} > 25-30\%$, there is an increase in the small pore diameter up to at least 18 nm; coincidently, a drop in the large pores diameter is observed. This effect can be ascribed to the enhanced solubility of PPG in THF. Considering the increasing pore diameter with V_{THF}, it appears that THF assists the dissolution of PPG inside the micelles that are formed at the mesoscopic scale upon solvent evaporation. These PPG-swollen micelles are efficient templates for the smaller mesopore population, which displays pore diameters larger than those usually observed in F127-templated titania thin films.[29] The presence of the larger pore population at low V_{THF} can be ascribed to a controlled phase separation triggered by the increasing concentration of PPG upon film drying. The partition of PPG between the forming micelles and the titania-solvent matrix upon film formation is also a key issue in determining the pore diameter of the large pore population. When PPG is essentially dissolved in the micelles, the phase separation process leading to the large pore population should be less abrupt, influencing the large pore size. The size of the larger pores should be thus controlled by the dynamics of two processes: the macroscopic phase separation and the increasing viscosity attained upon film formation and drying processes.[33,34] In addition, for higher

(33) Nakanishi, K. *J. Porous Mater.* **1997**, *4*, 67.
(34) Grosso, D.; Cagnol, F.; Soler-Illia, G. J. A. A.; Crepaldi, E. L.; Amenitsch, H.; Brunet-Bruneau, A.; Bourgeois, A.; Sanchez, C. *Adv. Funct. Mater.* **2004**, *14*, 309.

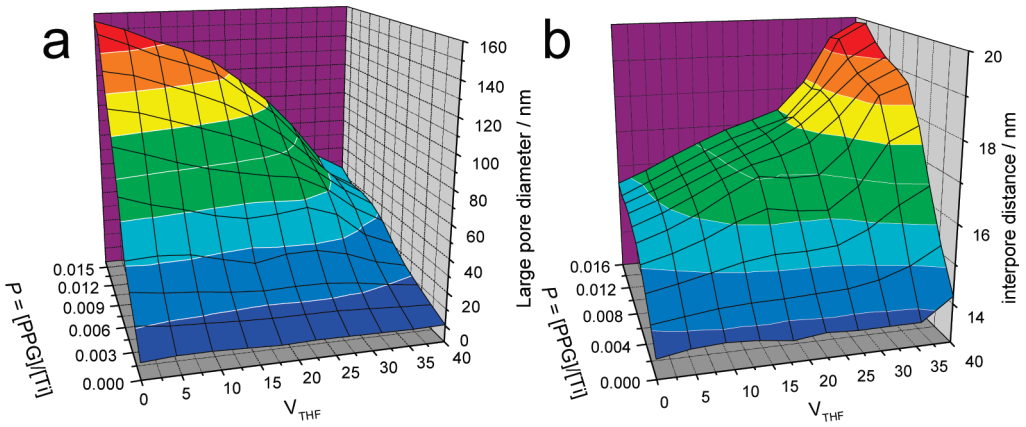

Figure 5. (a) Pore diameters and (b) interpore distances, for large and small pore populations respectively, obtained by SAXS and FE-SEM analysis of multiporous titania films calcined at 350 °C, as a function of synthesis parameters V_{THF} and P = [PPG]/[Ti] ($S = 4 \times 10^{-3}$).

V_{THF}, the co-solvent will be kept in solution for longer times, kinetically assisting the F127 swelling by PPG.

A complex process, where EISA and macroscopic phase separation run in parallel, appears to be responsible for the observed bimodal film texture. The balance between micelle formation and swelling, micelle organization, and macroscopic phase separation is a key point for the design of these films with multiporous textures. Figure 5 demonstrates that these features can be indeed controlled by adjusting external synthesis and processing parameters. In the precursor solution, PPG can play two different roles, depending on the co-solvent. The relatively high solubility of small size PPG molecules in a solvent with an intermediate hydrophobic character, such as THF (partition coefficients $P_{o/w}$ are 2.9 and 7.4 for THF and butanol, respectively),[35] leads to a complex behavior. In absence of the co-solvent, some of the PPG molecules enter the micelles and act as a pore swelling agent; the remaining PPG triggers demixing, originating the large mesopores observed. This phase separation process can take place by either an entropic or an enthalpic mechanism;[33] the collected data so far are not enough to discern between both alternatives. On the other hand, larger amounts of THF enhance the solubility of PPG in the micelles, even if it is not yet clear if PPG is located in the corona or the hydrophobic core. This leads to a higher swelling of the smaller pores; at the same time, less PPG is available in the extramicellar space. Therefore, phase separation is less likely, and the system tends to produce one pore size population. These two are examples of extreme conditions; in intermediate situations, we observed a combination of these possibilities. At this point, the combination of species of intermediate hydrophilic/hydrophobic behavior such as THF and moderate weight PPG appears very important, as far as it determines the dynamics of the evolution. Using this technique, we have obtained pore dimensions with the upper limit of around 200 nm. In principle, varying the hydrophobic character (either by changing the PPG size or the monomer) can lead to control of pore size in other length scales. We have also controlled how a higher content of THF in the absence of PPG can affect the porosity of the titania films; a higher dilution of the solution gives a thinner film with slightly larger mesopores, in good agreement with the literature.[9,10]

Scheme 1

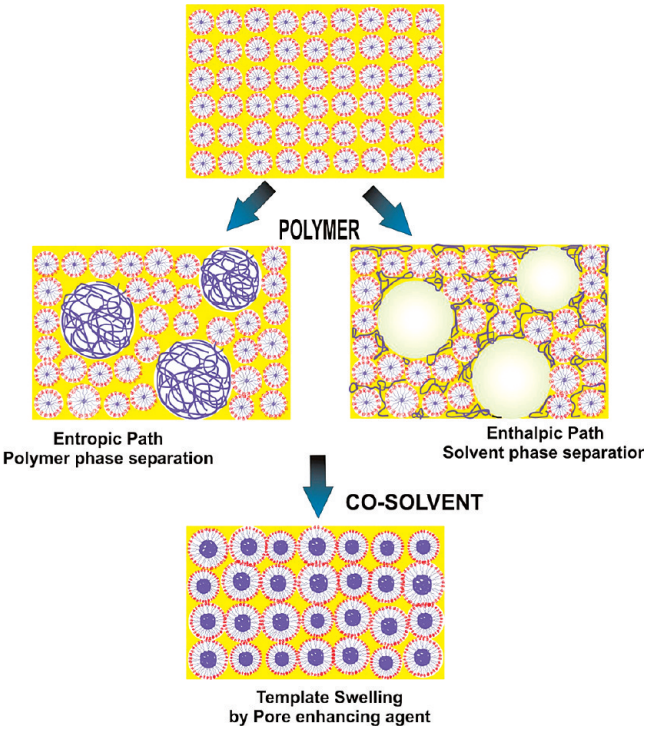

It is also important to stress that the method we have developed allows the production of robust, crack-free films and that the pores are interconnected and accessible from the external environment, as assessed by X-ray reflectivity experiments performed under different relative humidity (RH%) conditions (see Supporting Information). In the calcination temperature range explored so far, no anatase was detected by XRD of glass-supported films; however, it is known that a variable anatase fraction is present under these conditions for 10 nm pore mesoporous films, depending on the substrate.[26b] Experiments are planned to obtain large anatase fractions in due course.

(35) Sterner, O. Chemistry Health and the Environment; Wiley: Weinheim, 1999; p 42.

Conclusions

In summary, for the first time to our knowledge, a one-pot strategy is reported here that is capable of producing hierarchically nanoporous oxide thin films with highly and rationally controlled pore size and spatial distribution. This designed strategy permits the preparation of transparent titania thin films with hierarchical mesoporosity from commercially available, non-toxic templates and simple inorganic precursors. The straightforward preparation conditions reported mask a complex underlying physical−chemical process, which has to be systematically studied to obtain total control of the materials' features. The key point is mastering the balance among the co-assembly of the inorganic precursors, the supramolecular template, and the behavior of a pore enhancing agent such as PPG. The addition of PPG to alcohol/water solutions containing titania precursors and template results in the co-existence of smaller mesopores and large mesopores, which are produced by phase separation. Addition of a co-solvent of intermediate hydrophilicity such as THF assists the dissolution of PPG in the micelles, directing to a more uniform population of intermediate size mesopores (Scheme 1). An appropriate balance of PPG and THF permits the in situ generation of a tailored templating system with multiple characteristic lengths, obtained by controlling the phase separation and micellar template swelling behavior of a surfactant/polymer/solvent/co-solvent mixture.

The method presented here opens the gate for crossing the 10 nm barrier in mesoporous films and creating multimodal porous thin films with large mesopores, a necessary step for the immobilization of functional biomacromolecules (enzymes, antibodies, antigens, DNA or RNA fragments) in robust, accessible film matrixes,[6] as has been demonstrated in the case of mesocellular foams.[36] This route is a fast and reliable alternative to the more delicate and time-consuming film producing methods that use latex or silica beads as large pore molds, where repulsion between the colloidal templates should be adequately managed, and requires slow deposition followed by impregnation methods to obtain even materials.[12] In addition, colloidal templating has limitations regarding even film deposition on large area substrates.

The chemical strategy presented here relies on low-condensed, hydrophilic metal-oxo clusters and their interaction with low-weight polymers and supramolecular templates. We anticipate that this route can be extended readily to other oxides (silica, zirconia, ceria, and so forth) or hybrid materials, by adding organic functions to these cavities by pre- or postfunctionalization.[24,37] Finally, these methods can be easily combined with other patterning procedures to gain lateral resolution, leading to patterned hierarchical porous transparent films.[38]

Acknowledgment. Work financed by Ministero degli Affari Esteri "Progetti di grande Rilevanza", ITA-ARG collaboration, Grants FIRB 2003 (RBNE 033 KMA), ANPCyT (PICT 34518, PAE 2004 22711, RENAMSI), LNLS (D11A-SAXS1 projects #5755/07, #6721/07, #6729/07, #6666/07; D10A-XRD2 projects #6690/07 and #6698/07) and Gabbos (D&G 055). M.G.B. acknowledges a postdoctoral grant from CONICET. P. C. Angelomé and M. C. Fuertes are acknowledged for help in XRR and SAXS measurements; thanks are due to P. di Capri, P. Ortega, and D. Capussotto for inspiring discussions.

Supporting Information Available: Further details are given in Figures S1 and S2. This material is available free of charge via the Internet at http://pubs.acs.org.

(36) (a) Schmidt-Winkel, P.; Lukens, P. P.; Zhao, D. Y.; Yang, P.; Chmelka, B. F.; Stucky, G. D. *J. Am. Chem. Soc.* **1999**, *121*, 254. (b) Lettow, J. S.; Han, Y. H.; Schmidt-Winkel, P.; Yang, P.; Zhao, D. Y.; Stucky, G. D.; Ying, J. Y. *Langmuir* **2000**, *16*, 8291.

(37) (a) Sanchez, C.; Soler-Illia, G. J. A. A.; Ribot, F.; Grosso, D. *C. R. Acad. Sci.* **2003**, *6*, 1131. (b) Angelomé, P. C.; Soler-Illia, G. J. A. A. *J. Mater. Chem.* **2005**, *15*, 3903.

(38) Falcaro, P.; Costacurta, S.; Malfatti, L.; Takahashi, M.; Kidchob, T.; Casula, M. F.; Piccinini, M.; Marcelli, A.; Marmiroli, B.; Amenitsch, H.; Schiavuta, P.; Innocenzi, P. *Adv. Mater.* **2008**, *20*, 1864.